# Interaction of a bichromatically driven two-level atom with a squeezed vacuum: Photon statistics and squeezing

Matthias Jakob[1] and Gagik Yu. Kryuchkyan[1,2,3]
[1]*Abteilung für Quantenphysik, Universität Ulm, D-89069 Ulm, Germany*
[2]*Institute for Physical Research, National Academy of Sciences, 378410 Ashtarak-2, Armenia*
[3]*Yerevan State University, Alex Manookian 1, 375049 Yerevan, Armenia*
(Recieved 7 September 1999; published 19 April 2000)

We consider effects of a broadband squeezed reservoir on the second-order intensity correlation, and on squeezing properties in the resonance fluorescence of a bichromatically driven two-level atom in a cavity of moderate *Q*. Phase-dependent squeezed reservoir effects change the photon statistics, and lead to an amplification of the degree of squeezing. Squeezed reservoir effects in the second-order correlation function $g^{(2)}(\tau)$ are determined by two-photon emission processes which can be enhanced or suppressed in dependence on the squeezing phase.

PACS number(s): 42.50.Ar, 42.50.Dv

## I. INTRODUCTION

Atoms in squeezed light fields are of fundamental interest in atomic spectroscopy. This topic received a great stimulation when Gardiner [1] showed that the two dipole quadratures of a two-level atom in a squeezed vacuum field decay at different rates. Carmichael *et al.* [2,3] examined the influence of squeezed light on the resonance fluorescence of a single, monochromatically driven two-level atom, and an anomalous resonance fluorescence spectrum was predicted by Swain and co-workers [4–8]. Related problems in the absorption spectrum of a single monochromatically driven two-level atom have also been investigated [9–20]. A general overview about this topic was given in Ref. [21].

Squeezed reservoir effects in the resonance fluorescence spectrum of *bichromatically* driven two-level atoms were investigated in Refs. [22,23], and the Autler-Townes probe-field absorption spectrum was analyzed in Ref. [20]. However, effects of squeezed reservoirs on the photon correlation phenomenon as well as on squeezing properties in the resonance fluorescence of a *bichromatically* driven two-level atom have not yet been examined. On the other hand, these effects are well known in the photon statistics [24,25], and in the squeezing properties [25–28] of a *monochromatically* driven two-level atom. In view of recent experimental progresses in the detection of squeezing in resonance fluorescence, theoretical investigations of squeezing properties are still of interest [29–32], although the experimental verification of squeezing in the resonance fluorescence of a *single* atom has not yet been confirmed [29]. However, recently, Lu and co-workers [30–32] verified squeezing in the resonance fluorescence of a monochromatically driven *atomic beam* which is equivalent to squeezing properties of a single atom for scattering *in the forward direction* of the many-atom phase-dependent fluorescence spectra [33].

Most studies of squeezing properties in resonance fluorescence light considered a single two-level atom which is interacting with a *monochromatic* driving field. Theoretical investigations were performed on total squeezing [34–37], as well as on spectral component squeezing [37,38] in homodyne detection schemes. In contrast, intensity correlations and squeezing properties in the resonance fluorescence of a *bichromatically* driven two-level atom are not as familiar, although both already exhibit interesting features in an ordinary vacuum [39,40]. These properties differ distinctively from that of a monochromatically driven two-level atom. The most remarkable feature are possible two-photon emission processes which crucially depend on the strength of the atom-bichromatic field interaction. These two-photon emissions determine the unusual intensity correlations as well as the squeezing properties [39,40].

In this paper we discuss various aspects of squeezed reservoir effects in the bichromatically driven two-level atom: the second-order intensity correlation $g^{(2)}(\tau)$ and the spectrum of squeezing. In order to observe the squeezed reservoir effects, we take a cavity environment into account. The cavity environment is required, as it is impractical to squeeze all of the vacuum modes that interact with an atom. The simplest situation to examine is the *bad cavity limit*, which allows one to obtain an effective master equation. This effective master equation is formally equivalent to the free-space situation, but with cavity renormalized parameters [41–44]. Based on this model (also see Fig. 1), we derive analytical solutions for the second-order correlations as well as for the spectrum of squeezing. The assumptions which are necessary for an analytical treatment are symmetrically detuned field components $\omega_0+\delta$ and $\omega_0-\delta$ with respect to the atomic transition frequency $\omega_0$ of equal amplitudes. This allows us to introduce the *Floquet states* of the combined ''atom plus bichromatic field system,'' and to perform a secular approximation in the derivation of the master equation which is justified in the limit of resolved spectral linewidths. The squeezed reservoir may change the photon statistics from super- to sub-Poissonian statistics in dependence on the squeezing phase. This is naturally manifested in the second-order correlation function as well. In addition, the degree of squeezing in the resonance fluorescence can be enhanced or suppressed in dependence on the squeezing phase, similar to what occurs as in a monochromatic driving field case [27]. However, the enhancement of squeezing is not as strong as

 

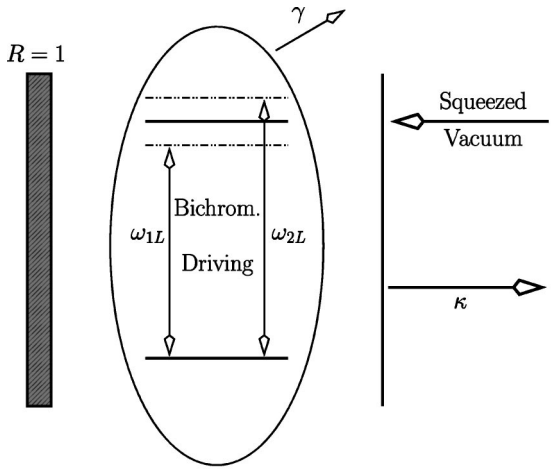


FIG. 1. A schematic representation of the physical system under consideration. A bichromatically driven two-level atom in a cavity is illuminated by a broadband squeezed vacuum through the (right) input mirror. The atom is pumped by the bichromatic field from the open sides of the cavity. The decay rate of the atom into different modes than the cavity modes is characterized by $\gamma$, while the cavity decay rate is denoted with $\kappa$.

in the monochromatic driving field case. All these features can be understood as the influence of a squeezed reservoir on the two-photon emission processes in the resonance fluorescence of a bichromatically driven two-level atom. In order to observe these squeezed reservoir effects, however, we have to point out that the bichromatic driving field as well as the squeezed vacuum field and, if we are interested in the squeezing properties, the local oscillator field has to be generated from a common laser source in order to maintain the phase relations between them. This is surely an experimental challenge, but it should be possible to realize. In particular, the bichromatic driving field can easily be realized with the help of an acousto-optical modulator, since it can be understood as a 100% amplitude-modulated field where the central component is suppressed.

This paper is organized as follows: In Sec. II we introduce the Floquet states of the combined ''two-level atom plus bichromatic field'' system. We derive the master equation in the Floquet state representation and the secular approximation. In Sec. III we consider squeezed reservoir effects on the second-order intensity correlation function. Section IV deals with the effects of a squeezed reservoir on the photon statistics based on the Mandel $Q$ parameter [45,46]. In Sec. V we consider squeezed reservoir effects on total squeezing, and in Sec. VI on the spectrum of squeezing. We conclude and summarize in Sec. VII.

## II. MASTER EQUATION IN FLOQUET-STATE REPRESENTATION

It is well known that the interaction of a two-level atom with a bichromatic driving field yields to Floquet states [47–50] or analogous dressed states [51]. These Floquet states have analytical expressions if the field consists of two components with *equal* amplitudes, and a relative phase $\Phi$ at frequencies $\omega_{1L}=\omega_0-\delta$ and $\omega_{2L}=\omega_0+\delta$, which are *symmetrically* detuned from the atomic transition frequency $\omega_0$:

$$E(t)=E_0\mathrm{Re}(e^{i\omega_{2L}t-2i\Phi}+e^{i\omega_{1L}t}). \tag{1}$$

Under these circumstances the Floquet states are given in the rotating-wave approximation as [47–50]

$$\begin{aligned}|\Phi_1(t)\rangle&=A_1(t)|\varphi_1\rangle-iA_2(t)e^{-i\omega_0 t}|\varphi_2\rangle,\\ |\Phi_2(t)\rangle&=-iA_2^*(t)|\varphi_1\rangle+A_1(t)e^{-i\omega_0 t}|\varphi_2\rangle,\\ A_1(t)&=\cos[(\xi/2)\sin(\delta t+\Phi)],\\ A_2(t)&=\sin[(\xi/2)\sin(\delta t+\Phi)]e^{-i\Phi}.\end{aligned} \tag{2}$$

Here $\xi=2V_0/(\hbar\delta)$ is the dimensionless interaction parameter with $V_0=|\vec{d}\cdot\vec{E}_0|$, $\vec{d}$ is the dipole moment of the atomic transition, and $|\varphi_1\rangle$ and $|\varphi_2\rangle$ denote the atomic ground and excited states, respectively.

Transitions between the Floquet states can be induced if the combined atom plus bichromatic field system interacts with an electromagnetic reservoir. The specific case we are interested in is the situation where the reservoir is in a squeezed vacuum state. In order to observe squeezed reservoir effects in free space, it is necessary to squeeze all of the vacuum modes that interact with an atom, a situation which is experimentally not feasible, although a few schemes were recently suggested which allows one to mimic such a squeezed reservoir environment by means of more convenient methods [52–54]. In contrast, the cavity environments where only those modes centered around the privileged cavity mode need be squeezed, provides a much more realistic scenario for an experimental investigation of squeezed reservoir effects. The two-level atom within the cavity is driven by the bichromatic field through the open sides of the cavity. In addition it is illuminated by the broadband squeezed vacuum through one mirror, as shown in Fig. 1.

The broadband squeezed reservoir is characterized by parameters $N$ and $M$ through relations between the creation and annihilation operators of the vacuum reservoir:

$$\begin{aligned}\langle a(\omega_1)a^\dagger(\omega_2)\rangle&=[N(\omega_1)+1]\delta(\omega_1-\omega_2),\\ \langle a(\omega_1)a(\omega_2)\rangle&=M(\omega_1)\delta(2\omega_S-\omega_1-\omega_2).\end{aligned} \tag{3}$$

Here $N(\omega_1)$ is the number of photons with frequency $\omega_1$ in the relevant mode of the reservoir, $M(\omega_1)=|M(\omega_1)|e^{i\theta}$ characterizes the photon correlations in the squeezed reservoir, and $\omega_S$ is the carrier frequency of the broadband squeezed field which is chosen to be $\omega_S=\omega_0$. The squeezing phase $\Psi$ is defined as

$$\Psi=\theta-2\Phi, \tag{4}$$

where $\Phi$ is the phase which appears in the bichromatic driving field. The magnitude $|M|=|M(\omega_0)|$ of photon correlations in the squeezed reservoir is bounded above by its value for a minimum uncertainty state and a given photon number

$N(\omega_0)$ in the squeezed reservoir. It is convenient to introduce a parameter $\eta$ where $0 \leqslant \eta \leqslant 1$, which enables us to write the relation

$$|M| = \eta[N(N+1)]^{1/2}. \tag{5}$$

The quantity $\eta$ measures the degree of two-photon correlations in the squeezed reservoir, i.e., the case $\eta = 1$ corresponds to the reservoir being in an ideal squeezed state. The cavity damping is characterized with the cavity-damping parameter $\kappa$, and the atom decays spontaneously by the damping rate $\gamma$ to the vacuum modes through the open sides of the cavity (see Fig. 1).

In this paper we are interested in the simplest situation to examine squeezed reservoir effects, i.e., the *bad cavity limit*. This allows us to obtain equations which are formally equivalent to the free-space situation, but with cavity-renormalized parameters [41–44]. The bad cavity limit is defined by the relations

$$\kappa \gg g \gg \gamma \quad \text{with} \quad C = g^2/\kappa\gamma \ \text{ finite}, \tag{6}$$

where $g$ denotes the coupling constant of the two-level atom with the cavity mode. In addition, we assume that $\delta \ll \kappa$, so that all of the atomic dynamics (governed by the Floquet states) occur within the decay rate $\kappa$. In the bad cavity limit the cavity field decay dominates, and the cavity field response to the continuum modes is much faster than that produced by its interaction with the atom. Thus the atom always experiences the cavity mode in the state produced by the vacuum reservoir. The assumption of a broadband squeezed input implies that the bandwidth of squeezing has to be large compared to the cavity damping rate $\kappa$. Although this assumption is difficult to realize experimentally, we restrict ourselves to examining this situation, as we are interested in analytical results. However, it seems to be worthwhile to investigate finite bandwidth effects in this system, since the characteristic two-photon emissions appear exclusively in the central peak component of the resonance fluorescence spectrum.

The system can be described by the following master equation, as can be shown by adiabatically eliminating the cavity-mode variables [41–44]:

$$\begin{aligned}\dot{\rho}_A = &-i[H(t),\rho_A] + \gamma_c(N+1)(2\sigma_-\rho_A\sigma_+ - \rho_A\sigma_+\sigma_- \\ &- \sigma_+\sigma_-\rho_A) + \gamma_c N(2\sigma_+\rho_A\sigma_- - \rho_A\sigma_-\sigma_+ - \sigma_-\sigma_+\rho_A) \\ &- \gamma_c M(2\sigma_+\rho_A\sigma_+ - \rho_A\sigma_+\sigma_+ - \sigma_+\sigma_+\rho_A) \\ &- \gamma_c M(2\sigma_-\rho_A\sigma_- - \rho_A\sigma_-\sigma_- - \sigma_-\sigma_-\rho_A) \\ &+ \gamma(2\sigma_-\rho_A\sigma_+ - \rho_A\sigma_+\sigma_- - \sigma_+\sigma_-\rho_A).\end{aligned} \tag{7}$$

Here $\sigma_+$ and $\sigma_-$ are the usual Pauli spin-$\frac{1}{2}$ operators, $\gamma_c = g^2/\kappa$, and $H(t)$ is given by

$$\begin{aligned}H(t) = &\frac{\omega_0}{2}\sigma_z + \frac{V_0}{2\hbar}\sigma_+[e^{i(\omega_0+\delta)t-2i\Phi} + e^{i(\omega_0-\delta)t}] \\ &+ \frac{V_0}{2\hbar}\sigma_-[e^{-i(\omega_0+\delta)t+2i\Phi} + e^{-i(\omega_0-\delta)t}],\end{aligned} \tag{8}$$

which describes the coherent evolution of the bichromatically driven two-level atom. We solve the master equation (7) in the interaction picture and in the Floquet-state basis [see Eq. (2)]. In addition, we adopt the secular approximation [$\delta \gg \gamma + \gamma_c = \tilde{\gamma}_c$, for a reservoir with mean photon number $N$: $\delta \gg (N+1)\gamma_c + \gamma$], which leads to similar results as in Ref. [23], where the free-space squeezed reservoir situation is treated. We rewrite the equations of motion for the reduced density matrix elements in the Floquet-state representation in the form $\sigma_{\alpha\beta}(t) = \langle \hat{\varrho}_{\alpha\beta}(t)\rangle = \langle \rho_A(t)|\beta\rangle\langle\alpha|\rangle$ where $|\alpha\rangle$ and $|\beta\rangle$ are the Floquet states of the system at $t=0$ [see Eq. (2)]. We obtain for the population elements [$\sigma_{\alpha\alpha}(t)$] and the transition elements [$\sigma_{\alpha\beta}(t)$, with $\alpha \neq \beta$]:

$$\dot{\sigma}_{11}(t) = -\Gamma_{11}(\sigma_{11}(t) - \sigma_{11}^S), \tag{9}$$

$$\dot{\sigma}_{12}(t) = -\Gamma_{12}\sigma_{12}(t). \tag{10}$$

Here $\sigma_{11}^S$ is the steady-state population of the Floquet state $|\Phi_1\rangle$. The decay rates $\Gamma_{12}$ and $\Gamma_{11}$, and the steady-state population inversion $\Delta$ obey

$$\begin{aligned}\Gamma_{12} = &\frac{\tilde{\gamma}_c}{8}[5 - J_0(2\xi)] + \frac{\tilde{\gamma}_c}{8}\left(\frac{C}{C+1}\right)\{2N[5 - J_0(2\xi)] \\ &+ 2|M|[1 - J_0(2\xi)]\cos\Psi\},\end{aligned} \tag{11}$$

$$\begin{aligned}\Gamma_{11} = &\tilde{\gamma}_c\left(\frac{C}{C+1}\right)\left[2N - \frac{1 - J_0(2\xi)}{2} \times \left(N + \frac{1}{2} + |M|\cos\Psi\right)\right] \\ &+ \tilde{\gamma}_c\left[1 - \frac{1 - J_0(2\xi)}{4}\right],\end{aligned} \tag{12}$$

$$\Delta = \sigma_{11}^S - \sigma_{22}^S = \tilde{\gamma}_c\frac{J_0(\xi)}{\Gamma_{11}}. \tag{13}$$

We recall that the squeezing phase $\Psi$ was defined in Eq. (4). In comparison to the free-space situation the master equation contains a cavity-modified decay rate $\gamma_c$. The factor $C/(1+C)$, with $C = \gamma_c/\gamma$, which appears in the above expressions, is the ratio of the spontaneous emission into the cavity mode to the total spontaneous decay rate $\tilde{\gamma}_c = \gamma(1+C)$. This quantity is sometimes referred to as the $\beta$ *value* $\beta = C/(1+C)$ of the cavity system [41–44].

We may introduce the following cavity-modified quantities $N_c$ and $M_c$ as *effective* squeezing parameters:

$$N_c = \frac{C}{1+C}N, \tag{14}$$

$$M_c = \frac{C}{1+C}M, \tag{15}$$

which are experienced by the atom in the bad cavity limit [41–44]: An important consequence of these expressions is the fact that we cannot have a perfectly correlated (minimum uncertainty) squeezing in the bad cavity limit [41–44]

$$|M_c| = \left[ N_c \left( N_c + \frac{C}{C+1} \right) \right]^{1/2} < [N_c(N_c+1)]^{1/2}. \quad (16)$$

When we define a cavity-modified squeezing parameter $\eta_c = M_c / [N_c(N_c+1)]^{1/2}$, we have

$$0 \leqslant \eta_c < 1. \quad (17)$$

Thus the squeezed reservoir in the bad cavity limit cannot be a perfectly correlated squeezed reservoir field, even when the input field into the cavity is in a perfectly correlated one. The effective degree of correlations are necessarily reduced from its value in the input-squeezed field as an effect of the remaining unsqueezed reservoir modes which the atom experiences through the open sides of the cavity.

### III. TWO-TIME INTENSITY CORRELATION FUNCTION

We express expectation values of the radiation field in terms of the positive- and negative-frequency parts of the Heisenberg-dipole moment operators $\mathcal{D}^{(+)}(t)$ and $\mathcal{D}^{(-)}(t)$ in the Floquet-state representation:

$$\mathcal{D}^{(-)}(t) = \sum_{\alpha\beta} \hat{\varrho}_{\alpha\beta}(t) d_{\alpha\beta}^{(-)}(t) = \frac{d}{2} \lambda(t) e^{-i\omega_0 t}, \quad (18)$$

$$\lambda(t) = [1 + C(t)] \hat{\varrho}_{12}(t) + e^{-2i\Phi} [1 - C(t)] \hat{\varrho}_{21}(t) + B(t) \times [\hat{\varrho}_{11}(t) - \hat{\varrho}_{22}(t)]. \quad (19)$$

Here the coefficients are given by

$$C(t) = 2A_1^2(t) - 1 = \cos[\xi \sin(\delta t + \Phi)], \quad (20)$$

$$B(t) = -2iA_1(t)A_2(t) = -ie^{-i\Phi} \sin[\xi \sin(\delta t + \Phi)]. \quad (21)$$

The matrix elements $d_{\alpha\beta}^{(\pm)}(t) = \langle \Phi_\alpha(t) | \hat{d} | \Phi_\beta(t) \rangle$ describe the positive- and negative-frequency parts of the dipole-moment in the Floquet-state representation.

The normalized second-order intensity correlation function $g^{(2)}(\tau)$ can be expressed as

$$g^{(2)}(t; t+\tau) = \frac{\langle \lambda^+(t) \lambda^+(t+\tau) \lambda(t+\tau) \lambda(t) \rangle}{\langle \lambda^+(t) \lambda(t) \rangle \langle \lambda^+(t+\tau) \lambda(t+\tau) \rangle}, \quad (22)$$

by taking into account the proportionality of the field operator in the far zone of the radiation field to the Heisenberg dipole-moment operator as well as Eqs. (18)–(21). The correlation function (22) can be investigated by applying the quantum regression theorem, and Eqs. (9) and (10). In the steady-state regime $t \gg \tilde{\gamma}_c$, for $g^{(2)}(\tau)$ we obtain, in a similar way as in Refs. [39,40]

$$g^{(2)}(\tau) = 1 + \frac{1}{F(\tau)} (F_1(\tau) e^{-\Gamma_{11}\tau} + F_2(\tau) e^{-\Gamma_{12}\tau}), \quad (23)$$

$$F(\tau) = 1 - 2\Delta J_0(\xi) + \frac{\Delta^2}{2} \left[ J_0\left( 2\xi \cos\frac{\delta\tau}{2} \right) + J_0\left( 2\xi \sin\frac{\delta\tau}{2} \right) \right], \quad (24)$$

$$F_1(\tau) = \frac{\Delta}{4} [J_0(\xi\sqrt{5 + 4\cos\delta\tau}) + J_0(\xi\sqrt{5 - 4\cos\delta\tau})] - \frac{1}{2}(1 + \Delta^2) \left[ J_0\left( 2\xi \cos\frac{\delta\tau}{2} \right) + J_0\left( 2\xi \sin\frac{\delta\tau}{2} \right) \right] + \frac{3}{2} J_0(\xi)\Delta, \quad (25)$$

$$F_2(\tau) = \frac{1}{2} \left[ J_0\left( 2\xi \cos\frac{\delta\tau}{2} \right) - J_0\left( 2\xi \sin\frac{\delta\tau}{2} \right) \right] - \frac{\Delta}{4} [J_0(\xi\sqrt{5 + 4\cos\delta\tau}) - J_0(\xi\sqrt{5 - 4\cos\delta\tau})]. \quad (26)$$

We may already expect that this result is formally equivalent to the result of the free-space situation in Refs. [39,40]. However, the decay rates $\Gamma_{11}$ and $\Gamma_{12}$, as well as the steady-state population inversion $\Delta$, which contain cavity modified decay rates, differ from the free-space situation. It is clear that the effects of the squeezed reservoir are manifested in these expressions.

The photon correlations in the resonance fluorescence of a bichromatically driven two-level atom were investigated in Refs. [39,40] for cases of the interaction with an usual vacuum and a thermal reservoir. Most remarkable are possible two-photon emission processes which may occur for particular interaction parameters $\xi$, leading to a strong superbunching effect $[g^{(2)}(\tau) > 2]$ at characteristic delay times $\tau$. This superbunching is a pure nonclassical effect which cannot be described within a classical theory as the condition $|g^{(2)}(0) - 1| > |g^{(2)}(\tau) - 1|$, which must be valid for all delay times $\tau$ within a classical theory, is violated [55]. The super bunching determines the unusual photon statistics and squeezing properties, and becomes strongly suppressed in the presence of a thermal bath in cases of very small interaction parameters $\xi$. We have shown [39,40] that the two-photon processes depend strongly on the steady-state population inversion $\Delta$, which is a comparatively complicated function of the interaction parameter $\xi$ in comparison to monochromatic driving field cases. In particular, unusual photon correlation effects appear whenever the absolute of the steady-state population inversion displays a local maximum ($|\Delta| = \max$). Therefore, we expect strong squeezed reservoir effects in the photon correlation phenomena if there exists a squeezing-induced local maximum in the absolute of the steady-state population inversion $|\Delta|$. Another main effect of the squeezed reservoir is reflected in the decay rates $\Gamma_{11}$ and $\Gamma_{12}$, which differ significantly from their values in a typical reservoir as well as a thermal reservoir.

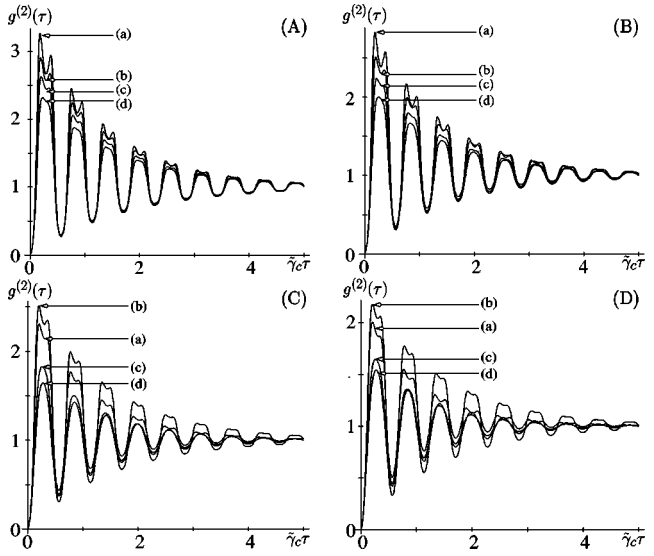


FIG. 2. Second-order correlation function in dependence on different reservoirs: (a) a squeezed reservoir with squeezing phase $\Psi=0$, (b) a typical vacuum, (c) a thermal reservoir, and (d) a squeezed reservoir with squeezing phase $\Psi=\pi$. The mean photon number $N$ and the interaction parameter $\xi$ are given as $N=0.015$ and $\xi=1$ in (A), $N=0.035$ and $\xi=1.2$ in (B), $N=0.15$ and $\xi=1.2$ in (C), and $N=0.25$ and $\xi=1.4$ in (D), and the photon correlations in the squeezed reservoir obey $|M|=[N(N+\beta)]^{1/2}$, with the $\beta$ value $\beta=C/(C+1)=10/11$. The detuning $\delta$ is given as $\delta=10\tilde{\gamma}_c$.

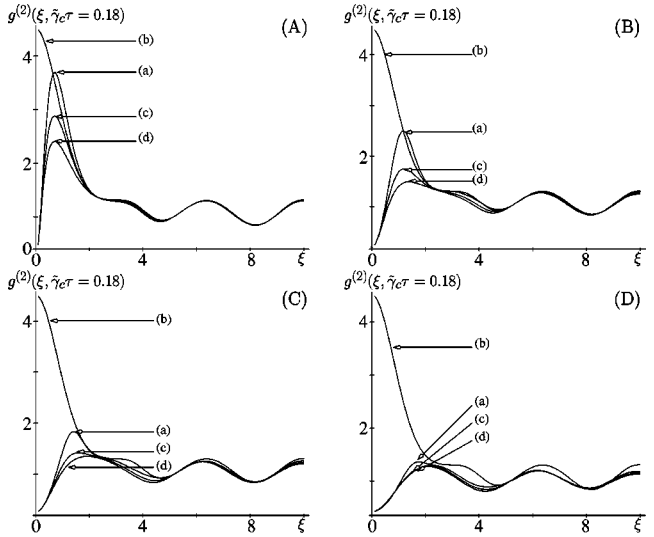


FIG. 3. Second-order correlation function in dependence on the interaction parameter $\xi$ and on different reservoirs at $\gamma\tau=0.18$: (a) a squeezed reservoir with squeezing phase $\Psi=0$, (b) a typical vacuum, (c) a thermal reservoir, and (d) a squeezed reservoir with squeezing phase $\Psi=\pi$. The mean photon number for the squeezed and thermal reservoirs are $N=0.01$ in (A), $N=0.1$ in (B) $N=0.3$ in (C), and $N=1$ in (D), and the photon correlations in the squeezed reservoir obey $|M|=[N(N+\beta)]^{1/2}$, with the $\beta$ value $\beta=C/(C+1)=10/11$. The detuning is given as $\delta=10\tilde{\gamma}_c$.

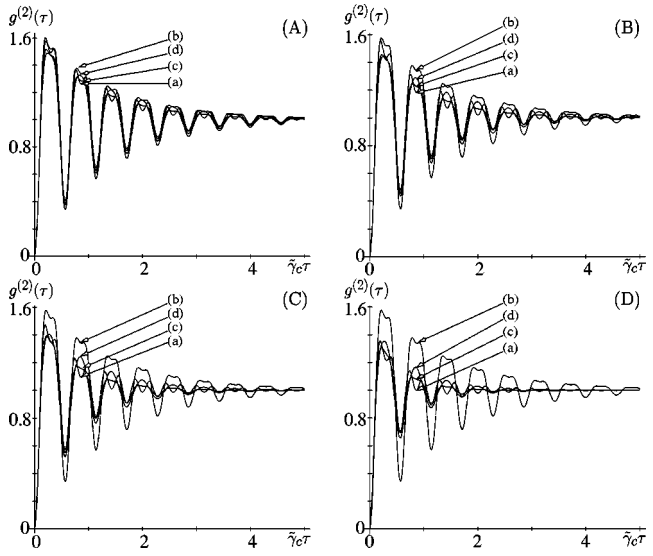


FIG. 4. Second-order correlation function in dependence on different reservoirs with interaction parameter $\xi=1.9$ and detuning $\delta=10\tilde{\gamma}_c$: (a) a squeezed reservoir with squeezing phase $\Psi=0$, (b) a typical vacuum, (c) a thermal reservoir, and (d) a squeezed reservoir with squeezing phase $\Psi=\pi$. The mean photon numbers $N$ obey $N=0.1$ in (A), $N=0.25$ in (B), $N=0.5$ in (C), and $N=1$ in (D), and the photon correlations in the squeezed reservoir are $|M|=[N(N+\beta)]^{1/2}$, with the $\beta$ value $\beta=C/(C+1)=10/11$.

We display the second-order correlation function $g^{(2)}(\tau)$ in dependence on different reservoirs and interaction parameters $\xi$ in Figs. 2–4. The strongest squeezed reservoir effects appear at small interaction parameters $\xi$ and small photon numbers $N$. It is remarkable that the squeezed reservoir can enhance or suppress the superbunching behavior in dependence on the squeezing phase $\Psi$, as shown in Figs. 2 and 3. In particular, a squeezing phase of $\Psi=0$ allows one to enhance the superbunching in the photon correlations, i.e., the two-photon emissions, while a squeezing phase of $\Psi=\pi$ allows one to suppress these two-photon emissions. The effects are, however, restricted to a particular range of interaction parameters $\xi$, and vanishes for larger numbers of photons in the reservoirs. This is shown in Fig. 3, where we display the first maximum of the second-order correlation in dependence on different reservoirs and interaction parameters $\xi$. The most obvious features of squeezed reservoir effects on the photon correlations can be summarized as follows: First, the squeezed reservoir effects are most pronounced for interaction parameters $\xi$ approximately between $1\leqslant\xi/\delta\leqslant 2$. In this interaction range the differences in the steady-state population inversion $\Delta$ become largest and, in particular, $|\Delta|$ displays a local maximum induced by the squeezed reservoir with squeezing phase $\Psi=0$, as shown in Fig. 5. This explains the enhancement of two-photon emissions in the resonance fluorescence. Second, the absolute of the steady-state population inversion $|\Delta|$ becomes reduced in the squeezed reservoir with squeezing phase $\Psi=\pi$ (again see Fig. 5), explaining the suppression of two-photon emissions in the photon correlations. In addition, the range of interaction parameters $\xi$ where squeezed reservoir effects occur depends on the photon number, i.e., for a larger number

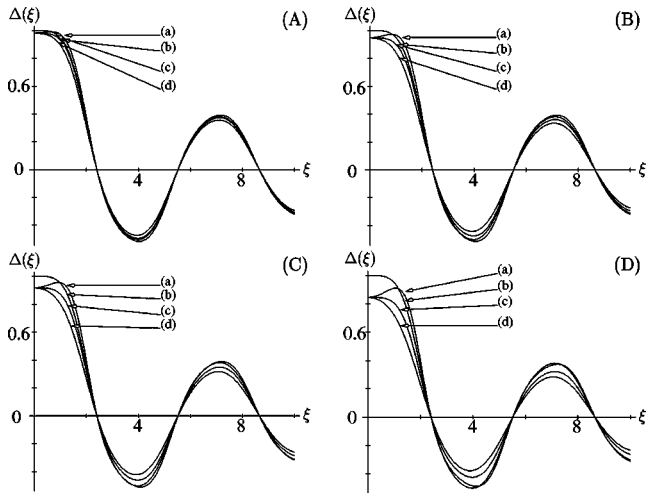


FIG. 5. Steady-state population inversion $\Delta$ in dependence on the interaction parameter $\xi$ and on different reservoirs with detuning $\delta=10\tilde{\gamma}_c$: (a) a squeezed reservoir with squeezing phase $\Psi=0$, (b) a typical vacuum, (c) a thermal reservoir, and (d) a squeezed reservoir with squeezing phase $\Psi=\pi$. The mean photon number $N$ is $N=0.01$ in (A), $N=0.03$ in (B), $N=0.05$ in (C), and $N=0.1$ in (D), and the photon correlations in the squeezed reservoir are $|M|=[N(N+\beta)]^{1/2}$, with the beta value $\beta=C/(C+1)=10/11$.

of photons in the squeezed reservoir the squeezed reservoir effects become less and less important, and more interestingly are shifted into ranges of stronger interaction parameters.

In Fig. 4 we display the second-order correlation function at interaction parameters $\xi$, where squeezed reservoir effects in the decay rates $\Gamma_{11}$ and $\Gamma_{12}$ become most pronounced. We realize that the fast oscillations in the second-order correlation function can be dramatically damped in dependence on the squeezing phase $\Psi$, especially for $\Psi=\pi$. On the other hand, these oscillations can be enhanced in the presence of a squeezed reservoir with squeezing phase $\Psi=0$. In this interaction range and at comparatively large photon numbers, the differences between thermal and squeezed reservoirs are less obvious. Nevertheless the dependence on the squeezing phase $\Psi$ of the second-order correlation function persists even for a large number of reservoir photons, as shown in Fig. 4. In this context, we remark that usually effects of a squeezed reservoir becomes negligible for a large squeezing phase $\Psi=\pi$, with an exception discussed in Ref. [56].

## IV. PHOTON STATISTICS

The second-order correlation function exhibits interesting properties in dependence on the field strength and on reservoir properties, as we have shown already. Thus we expect squeezed reservoir effects on the photon-counting statistics as well. The second-order correlation function allows one to analyze the mean-squared fluctuations in the photon number and, consequently, to determine whether the photon statistics are sub- or super-Poissonian. This decision can be made with the help of the Mandel $Q$ factor [45,46] which describes the deviation of the variance of the photon number $V(N)=\langle N^2\rangle-\langle N\rangle^2$ from a Poissonian variance. The Mandel $Q$ factor is defined as [45,46]

$$Q=\frac{V(N)-\langle N\rangle}{\langle N\rangle}=\frac{\langle N\rangle}{\gamma T}\Theta(\gamma T), \tag{27}$$

where

$$\Theta(T)=\int_{-T}^{T}d\tau\left(1-\frac{|\tau|}{T}\right)[g^{(2)}(\tau)-1]. \tag{28}$$

Here $T$ is the counting time interval during which photons are collected. The Mandel $Q$ factor $\Theta(T)$ is larger than zero if the photon statistics are super-Poissonian, zero, if the statistics are Poissonian, and smaller than zero if the statistics are sub-Poissonian.

It is quite obvious to connect super-Poissonian photon statistics with two-photon emissions into the resonance fluorescence [39,40]. The contribution of these two-photon processes is dominant in $g^{(2)}(\tau)$ if the absolute of the steady-state population inversion $|\Delta|$ displays a maximum in dependence on $\xi$ [39,40]. Thus squeezed reservoir effects in the photon-counting statistics are manifested in the steady-state population inversion $\Delta$, which can be strongly manipulated in the presence of a squeezed reservoir, as shown in Figs. 5. Interestingly, there are ranges of interaction parameters $\xi$ where it is possible to change the photon statistics from super- to sub-Poissonian in dependence on the squeezing phase $\Psi$. In particular, the photon statistics become sub-Poissonian due to the presence of a squeezed reservoir with a squeezing phase $\Psi=\pi$, while the photon statistics are super-Poissonian in squeezed reservoirs with a squeezing phase $\Psi=0$, as well as in thermal reservoirs and a usual vacuum. This is displayed in Table I.

TABLE I. The normalized Mandel $Q$ parameter $\Theta(T)$ in dependence on different reservoirs, a usual vacuum (UV), a thermal reservoir (TR), a squeezed reservoir with squeezing phase $\Psi=0$ (SR-$\Psi=0$), and a squeezed reservoir with squeezing phase $\Psi=\pi$ (SR-$\Psi=\pi$). We recognize parameters in which phase-dependent squeezed reservoir effects completely change the photon statistics.

| Parameters | UV | TR | SR-$\Psi=0$ | SR-$\Psi=\pi$ |
|---|---|---|---|---|
| $\xi=1.0$, $N=0.01$ | 1.77 | 1.50 | 2.23 | 1.04 |
| $\xi=1.9$, $N=0.01$ | 0.22 | 0.12 | 0.34 | 0.04 |
| $\xi=1.0$, $N=0.1$ | 1.77 | 0.33 | 1.20 | −0.02 |
| $\xi=1.2$, $N=0.1$ | 1.37 | 0.43 | 1.45 | 0.07 |
| $\xi=1.9$, $N=0.1$ | 0.22 | 0.12 | 0.34 | 0.04 |
| $\xi=1.0$, $N=0.25$ | 1.77 | −0.19 | 0.20 | −0.32 |
| $\xi=1.4$, $N=0.25$ | 0.97 | 0.07 | 0.78 | −0.10 |
| $\xi=1.9$, $N=0.25$ | 0.22 | 0.04 | 0.28 | −0.02 |
| $\xi=1.0$, $N=0.5$ | 1.77 | −0.36 | −0.26 | −0.37 |
| $\xi=1.4$, $N=0.5$ | 0.97 | −0.11 | 0.25 | −0.16 |
| $\xi=1.5$, $N=0.5$ | 0.79 | −0.08 | 0.78 | −0.10 |
| $\xi=1.9$, $N=0.5$ | 0.22 | −0.02 | 0.16 | −0.04 |

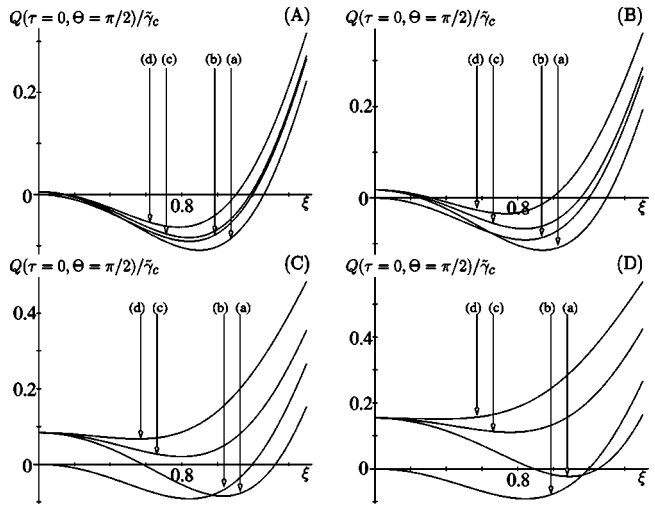


FIG. 6. Total squeezing in dependence on the interaction parameter $\xi$ and on different reservoirs with detuning $\delta/\tilde{\gamma}_c=10$: (a) a squeezed reservoir with squeezing phase $\Psi=0$, (b) a typical vacuum, (c) a thermal reservoir, and (d) a squeezed reservoir with squeezing phase $\Psi=\pi$. The mean photon numbers are $N=0.003$ in (A), $N=0.01$ in (B), $N=0.05$ in (C), and $N=0.1$ in (D), and the photon correlations in the squeezed reservoir obey $|M|=[N(N+\beta)]^{1/2}$, with the $\beta$ value $\beta=C/(1+C)=10/11$.

It is clear that for larger photon numbers squeezed reservoir effects become negligible in comparison to thermal reservoir effects. For large photon numbers the photon statistics in the resonance fluorescence are sub-Poissonian, independent of the reservoirs. This, again, is a result of the behavior of the steady-state population inversion $|\Delta|$, which is comparatively small in reservoirs with large photon numbers regardless what kind of reservoir is present. Consequently, two-photon emissions into the resonance fluorescence are suppressed. The change from super- to sub-Poissonian statistics is again an effect of a large squeezing phase $\Psi=\pi$, which is generally unusual in squeezed reservoirs [56].

## V. TOTAL SQUEEZING IN THE RESONANCE LIGHT

In this section we are interested in the situation where squeezing is detected in terms of normally ordered variances of the phase quadratures, which requires a direct homodyning of the total radiation field as a local oscillator without frequency filtering [57]. We denote this type of squeezing as total squeezing. An alternative detection scheme which measures the squeezing spectrum requires the fluorescent field to be first frequency filtered and then homodyned with a strong local oscillator field [30–32]. This situation is generally known as spectral component squeezing, and will be the subject of Sec. III.

Squeezing in the signal beam is conveniently connected with the normalized intensity correlation function $Q(\tau,\Theta)$, which can be expressed as [37,46]

$$Q(\tau,\Theta)=[\langle\Delta E^{(-)}(t)\Delta E^{(+)}(t+\tau)\rangle e^{i\omega_0\tau}+\langle\Delta E^{(-)}(t)\Delta E^{(-)}(t+\tau)\rangle\times e^{-i[\omega_0(2t+\tau)-2\Theta]}+\text{c.c.}], \tag{29}$$

where $\Delta E=E-\langle E\rangle$. Total squeezing occurs whenever $Q(\tau=0,\Theta)$ is smaller than zero [36]. The time evolution of $Q(\tau,\Theta)$ describes the progressive loss of negative correlations with increasing delay time. Thus a knowledge of the functional form of $Q(\tau,\Theta)$ allows one to calculate effects of finite detection times on measurable squeezing [36]. More interesting, the Fourier transformation of $Q(\tau,\Theta)$ determines the spectral component squeezing of the signal field [37],

$$\Psi(\omega,\Theta)=\int_{-\infty}^{\infty}Q(\tau,\Theta)e^{i\omega\tau}d\tau, \tag{30}$$

in dependence on the relative angle $\Theta$. Spectral component squeezing is obtained if $\Psi(\omega,\Theta)<0$ for appropriate values of $\omega$ and the phase $\Theta$ of the local oscillator [37], and will be the subject of Sec. VI.

We express Eq. (29) in terms of the Heisenberg dipole-moment operators (18) and (19), and under the assumption of the secular approximation derive, for $Q(\tau,\Theta)$,

$$Q(\tau,\Theta)=\frac{\tilde{\gamma}_c}{2}([1+\overline{C(t)C(t+\tau)}-2\Delta J_0(\xi)]e^{-\Gamma_{12}\tau}+\overline{B^*(t)B(t+\tau)}(1-\Delta^2)e^{-\Gamma_{11}\tau}+\cos(2\Theta)\times\{[1-\overline{C(t)C(t+\tau)}]e^{-\Gamma_{12}\tau}-\overline{B^*(t)B(t+\tau)}\times(1-\Delta^2)e^{-\Gamma_{11}\tau}\}), \tag{31}$$

where $Q(\tau,\Theta)$ is renormalized to the total outgoing flux $\tilde{\gamma}_c$ of the resonance fluorescence light, as usually [25,27,38,58]. The overline denotes averaging over the fast oscillations proportional to $\delta$ or multiplies of $\delta$ with respect to $t$, and

$$\overline{C(t)C(t+\tau)}=\frac{1}{2}\left\{J_0\left[2\xi\cos\left(\delta\frac{\tau}{2}\right)\right]+J_0\left[2\xi\sin\left(\delta\frac{\tau}{2}\right)\right]\right\},$$

$$\overline{B^*(t)B(t+\tau)}=\frac{1}{2}\left\{J_0\left[2\xi\sin\left(\delta\frac{\tau}{2}\right)\right]-J_0\left[2\xi\cos\left(\delta\frac{\tau}{2}\right)\right]\right\}.$$

We consider the two quadrature components of the signal field in phase ($\Theta=0$) or out of phase ($\Theta=\pi/2$) to the strong local oscillator, and, for $Q(\tau=0,\Theta=\pi/2)$, i.e., the out-of-phase component, we obtain

$$Q\left(\tau=0,\Theta=\frac{\pi}{2}\right)=\frac{\tilde{\gamma}_c}{2}\{2-2\Delta J_0(\xi)-\Delta^2[1-J_0(2\xi)]\}. \tag{32}$$

Similarly, for the in-phase quadrature element of the signal field, we derive

$$Q(\tau=0,\Theta=0)=\tilde{\gamma}_c[1-\Delta J_0(\xi)]. \tag{33}$$

The in-phase quadrature component of the signal field (33) cannot be squeezed regardless of what kind of reservoir is present. However, the out-of-phase component (32) displays squeezing.

We have plotted the normalized total squeezing in dependence on $\xi$ and different reservoirs in Figs. 6. Total squeez-

ing occurs in a range of small dimensionless interaction parameter $\xi/\gamma$. Interestingly, in the presence of a squeezed reservoir with $\Psi=0$, total squeezing can be enhanced, and the range of interaction parameters $\xi$ in which total squeezing occurs can also be enlarged. This is possible for small photon numbers $N$, and is vanishing for larger photon numbers. In comparison, total squeezing can be greatly suppressed in the presence of a squeezed reservoir with a squeezing phase $\Psi=\pi$. The differences in total squeezing occur due to the influences of the different reservoirs on the steady-state population inversion $\Delta$ (see Fig. 5). The steady-state population inversion $\Delta$ is responsible for two-photon emission processes which determine the squeezing properties in the resonance fluorescence. The presence of a thermal reservoir, and especially of a squeezed reservoir with squeezing phase $\Psi=\pi$, strongly suppresses the probability of two-photon emissions, leading to a decrease of total squeezing, as shown in Figs. 6. In contrast, these two-photon emissions can become more pronounced in a squeezed reservoir with $\Psi=0$, and this is responsible for the enhancement of the squeezing effects.

Another important feature in connection of measurable total squeezing is the temporal behavior of the relevant normalized correlation function $Q(\tau,\Theta)$, which allows one to consider questions of influences of finite detection times on squeezing [36]. The temporal correlation function out of phase to the strong local oscillator is given as

$$Q\left(\tau,\Theta=\frac{\pi}{2}\right)=\tilde{\gamma}_c[(\overline{C(t)C(t+\tau)}-\Delta J_0(\xi))e^{-\Gamma_{12}\tau} + \overline{B^*(t)B(t+\tau)}(1-\Delta^2)e^{-\Gamma_{11}\tau}]. \tag{34}$$

We recognize fast oscillations of the order of $\delta/2$ in the correlation function in dependence on $\tau$ (see Fig. 7). In particular, the correlation function becomes much more negative for $\tau\approx 2/\delta$ in comparison to $\tau=0$. Such a behavior has a positive consequence on the observation of squeezing in resonance fluorescence if we take finite detection times into account. These oscillations can be greatly enhanced or suppressed in the presence of a squeezed reservoir in dependence on the squeezing phase $\Psi$. Here again, the effects of the squeezed reservoir are most pronounced for small photon numbers as well as in a range of small interaction parameters, as shown in Fig. 7. The oscillations are manifestations of two-photon emission processes which can be amplified or suppressed in dependence on the squeezing phase $\Psi$ of the squeezed reservoir. It is important that this behavior of the correlation function is absent in the resonance fluorescence of a monochromatically driven atom. Here the temporal behavior of the correlation function is determined by the Rabi-frequency, which has to be smaller than the decay rate $\gamma$ in order to observe squeezing. Consequently no oscillations occur during a time interval $1/\gamma$ [37].

## VI. SPECTRAL COMPONENT SQUEEZING

In this section we investigate squeezed reservoir effects on the spectrum of squeezing, and if the degree of squeezing

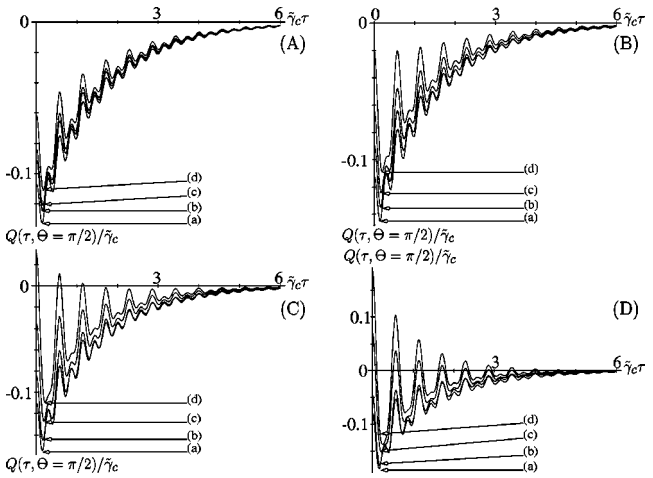


FIG. 7. Temporal behavior of $Q(\tau,\Theta=\pi/2)/\tilde{\gamma}_c$ in dependence on different reservoirs with detuning $\delta/\tilde{\gamma}_c=10$: (a) a squeezed reservoir with squeezing phase $\Psi=0$, (b) a typical vacuum, (c) a thermal bath, and (d) a squeezed reservoir with squeezing phase $\Psi=\pi$. The mean photon numbers in the reservoirs and the interaction parameter $\xi$ are given as $\xi=0.85$ and $N=0.003$ in (A), $\xi=0.9$ and $N=0.01$ in (B), $\xi=0.95$ and $N=0.02$ in (C), and $\xi=1.1$ and $N=0.05$ in (D), and the photon correlations in the squeezed reservoir obey $|M|=[N(N+\beta)]^{1/2}$, with the $\beta$ value $\beta=C/(C+1)=10/11$.

can be enhanced (or suppressed) in the presence of a squeezed reservoir. The normalized, dimensionless spectral component squeezing for $\Theta=\pi/2$ out of phase to the strong local oscillator, which we denote as $\Phi_{22}(\omega)$ and which is given as the Fourier transform of $Q(\tau,\Theta=\pi/2)$, provides for a measure of the degree of squeezing:

$$\Phi_{22}(\omega)=\int d\tau e^{i\omega\tau}Q\left(\tau,\Theta=\frac{\pi}{2}\right) = \sum_{q=-\infty}^{+\infty}[J_{2q}^2(\xi)-\delta_{q,0}\Delta J_0(\xi)] \times\frac{2\Gamma_{12}\tilde{\gamma}_c}{(\omega-2q\delta)^2+\Gamma_{12}^2}+\sum_{q=-\infty}^{+\infty}J_{2q+1}^2(\xi) \times(1-\Delta^2)\frac{2\Gamma_{11}\tilde{\gamma}_c}{[\omega-(2q+1)\delta]^2+\Gamma_{11}^2}. \tag{35}$$

We recognize that spectral component squeezing occurs exclusively in the central component $\omega=0$ of the resonance fluorescence spectrum. When we take into account the secular approximation condition $\delta\gg\tilde{\gamma}_c$ we may reduce Eq. (35), around the frequency $\omega=0$, into

$$\Phi_{22}(0)\approx 2[J_0^2(\xi)-\Delta J_0(\xi)](\tilde{\gamma}_c/\Gamma_{12}). \tag{36}$$

We display $\Phi_{22}(0)$ in dependence of $\xi$ and on different reservoirs in Fig. 8. The spectral component squeezing displays a similar dependence on the interaction parameter $\xi$ as the probability of two-photon emission processes does, i.e., the

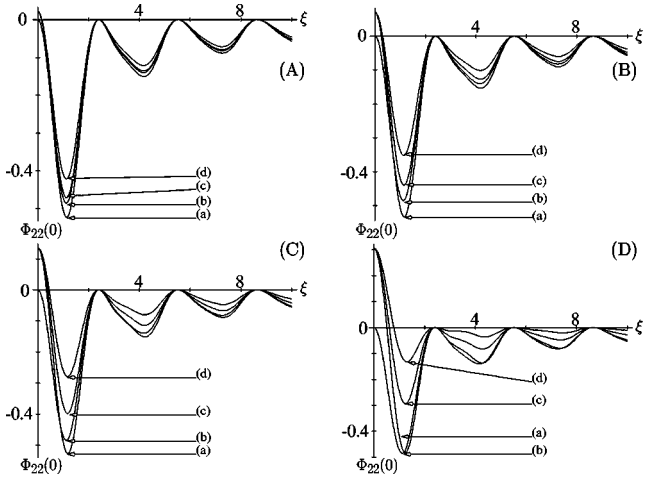


FIG. 8. Spectral component squeezing $\Phi_{22}(\omega=0)$ in dependence on the interaction parameter $\xi$ and on different reservoirs: (a) a squeezed reservoir with squeezing phase $\Psi=0$, (b) a typical vacuum, (c) a thermal reservoir, and (d) a squeezed reservoir with squeezing phase $\Psi=\pi$. The photon number in the squeezed an thermal reservoirs obey (A) $N=0.003$, (B) $N=0.01$, (C) $N=0.02$, and (D) $N=0.05$, and the photon correlations in the squeezed reservoir are $|M|=[N(N+\beta)]^{1/2}$, with the $\beta$ value $\beta=C(C+1)=10/11$.

steady-state population inversion $\Delta$ shows the same dependence on the interaction parameter $\xi$ [39,40]. This is the strongest evidence to connect the squeezing properties with the two-photon emission processes into the central component of the resonance fluorescence. In this context it is clear that spectral component squeezing can only be observed in the central peak of the spectrum. Thus it seems to be of particular interest to consider finite bandwidth effects of the squeezed reservoir on squeezing properties of the resonance fluorescence, however, this is not the subject of this paper. We recall that this behavior is in contrast to squeezing properties in the resonance fluorescence of a monochromatically driven atom, where the frequency range of the spectral component squeezing depends strongly on the interaction parameter $\xi$, i.e., the Rabi frequency [37].

We are interested in the effects of different reservoirs on spectral component squeezing of the out-of-phase quadrature component. Again, phase-dependent squeezed reservoir effects allow one to enhance or suppress the magnitude of squeezing in dependence on the squeezing phase $\Psi$, especially in the range of small photon numbers. This is similar to squeezed reservoir effects on squeezing properties of a monochromatically driven two-level atom [27]. However, the squeezed reservoir cannot enhance the degree of squeezing as strongly as in the monochromatic driving field case. The effects of squeezed and thermal reservoirs are shown in Fig. 8. Because thermal and squeezed reservoir effects lead to a dropping of the strong superbunching behavior for very small interaction parameters $\xi$, and, therefore, to a termination of the two-photon emissions, we expect no squeezing. This is demonstrated in Fig. 8 where the spectral component squeezing is plotted in thermal and squeezed reservoirs for different photon numbers as a function of $\xi$. Further, for stronger interaction parameters $\xi>2.5$ the effects of thermal and squeezed reservoirs on spectral component squeezing become negligible. More interestingly, we can enhance the degree of squeezing in the presence of a squeezed reservoir with a squeezing phase $\Psi=0$ for certain interaction parameters and small photon numbers, as shown in Figs. 8. In contrast the degree of squeezing can be strongly suppressed in the case of a squeezing phase of $\Psi=\pi$. These properties, again, can be understood as effects of the squeezed reservoir on the steady-state population inversion $\Delta$ which determines the probability of two-photon emission into the resonance fluorescence which are responsible for the squeezing properties.

We finally note that the normalized spectral component squeezing $\Phi_{11}(\omega)$ of the quadrature component in phase with the strong, local oscillator,

$$\Phi_{11}(\omega)=2[1-\Delta J_0(\xi)][(\Gamma_{12}\tilde{\gamma}_c)/(\omega^2+\Gamma_{12}^2)], \quad (37)$$

cannot be squeezed in the whole frequency range regardless of what kind of reservoir is present, and regardless of the interaction parameter $\xi$. The effects of the squeezed reservoir on this component are therefore not of particular interest.

## VII. SUMMARY AND CONCLUSIONS

We have studied squeezed reservoir effects on quantum statistical and squeezing properties of the resonance fluorescence of a single, bichromatically driven two-level atom. We have shown significant influences of a squeezed reservoir on the photon correlation phenomena, on photon-counting statistics, and on squeezing properties which depend on the mean number of photons in the cavity and on the interaction parameter $\xi$ of the bichromatic atom-field interaction. We further demonstrated the influence of a squeezed reservoir on the degree of squeezing, and showed that a squeezed reservoir allows one to enhance or suppress the degree of squeezing in the resonance fluorescence in dependence on the squeezing phase $\Psi$. Manipulations of the steady-state population inversion by different reservoirs are responsible for all these effects. The steady-state population inversion determines the probability of two-photon emissions in the resonance fluorescence and these two-photon emissions specify all nonclassical effects in the resonance light emitted by the bichromatically driven two-level atom. Further effects are manifested by the influences of different reservoirs on the decay rates of the Floquet states. Interestingly, these effects remain even for a large squeezing phase $\Psi=\pi$, which is generally unusual in squeezed reservoirs.

With respect to the recent experiment of Turchette *et al.* [59], who realized the atom-squeezed-vacuum interaction in the bad cavity limit, the proposed squeezed reservoir effects on photon correlations as well as on squeezing properties should be realizable. There it was also shown that many squeezed reservoir effects in the free-space situation can be carried over to the cavity situation in the bad cavity limit. Thus they verified in some sense the formally identical master equation of the free-space squeezed reservoir and the

cavity-modified squeezed reservoir situation in the bad cavity limit. However, we have to stress again that the driving fields as well as the squeezed vacuum field have to be generated from a common laser source in order to maintain the phase relations between them necessary for the observation of the squeezed reservoir effects.

**ACKNOWLEDGMENTS**

One of us (G.Yu.K.) appreciates the support of W.P. Schleich during his stay at the Universität Ulm. M.J. gratefully acknowledges the support of the Deutsche Forschungsgemeinschaft.

[1] C. W. Gardiner, Phys. Rev. Lett. **56**, 1917 (1986).
[2] H. J. Carmichael, A. S. Lane, and D. F. Walls, Phys. Rev. Lett. **58**, 2539 (1987).
[3] H. J. Carmichael, A. S. Lane, and D. F. Walls, J. Mod. Opt. **34**, 821 (1987).
[4] S. Smart and S. Swain, Phys. Rev. A **48**, R50 (1993).
[5] S. Swain, Phys. Rev. Lett. **73**, 1493 (1994).
[6] S. Swain and P. Zhou, Phys. Rev. A **52**, 4845 (1995).
[7] W. S. Smyth, S. Swain, Z. Ficek, and M. Scott, Phys. Rev. A **57**, 585 (1998).
[8] W. S. Smyth and S. Swain, Phys. Rev. A **59**, R2579 (1999).
[9] H. Ritsch and P. Zoller, Opt. Commun. **64**, 523 (1987).
[10] S. An, M. Sargent, and D. F. Walls, Opt. Commun. **67**, 373 (1988).
[11] Z. Ficek and B. J. Dalton, Opt. Commun. **102**, 231 (1993).
[12] Z. Ficek, W. S. Smyth, and S. Swain, Opt. Commun. **110**, 555 (1994).
[13] Z. Ficek, W. S. Smyth, and S. Swain, Phys. Rev. A **52**, 4126 (1995).
[14] S. S. Hassan, O. M. Frege, and N. Nayak, J. Opt. Soc. Am. B **12**, 1177 (1995).
[15] P. Zhou, Z. Ficek, and S. Swain, J. Opt. Soc. Am. B **13**, 768 (1996).
[16] P. Zhou and S. Swain, Quantum Semiclassic. Opt. **8**, 959 (1996).
[17] P. Zhou and S. Swain, Phys. Rev. A **55**, 772 (1997).
[18] M. Bosticky, Z. Ficek, and B. J. Dalton, Phys. Rev. A **53**, 4439 (1996).
[19] M. Bosticky, Z. Ficek, and B. J. Dalton, Phys. Rev. A **57**, 3869 (1998).
[20] M. Jakob and G. Yu. Kryuchkyan, Phys. Rev. A **57**, 1355 (1998).
[21] B. J. Dalton, Z. Ficek, and S. Swain, J. Mod. Opt. **46**, 379 (1999), and references therein.
[22] P. Zhou, S. Swain, and Z. Ficek, Phys. Rev. A **55**, 2340 (1997).
[23] G. Yu. Kryuchkyan, Zh. Éksp. Teor. Fiz. **109**, 116 (1996) [Sov. Phys. JETP **82**, 60 (1996)].
[24] R. D'Souza, A. S. Jayarao, and S. V. Lawande, Phys. Rev. A **41**, 4083 (1990).
[25] P. R. Rice and C. A. Baird, Phys. Rev. A **53**, 3633 (1996).
[26] S. Swain and P. Zhou, Opt. Commun. **123**, 310 (1996).
[27] Z. Ficek and S. Swain, J. Opt. Soc. Am. B **14**, 258 (1997).
[28] P. Zhou and S. Swain, Phys. Rev. A **59**, 3745 (1999).
[29] J. F. Höffges, H. W. Baldauf, T. Eichler, S. R. Helmfrid, and H. Walther, Opt. Commun. **133**, 170 (1997).
[30] H. Z. Zhao, Z. H. Lu, and J. E. Thomas, Phys. Rev. Lett. **79**, 613 (1997).
[31] H. Z. Zhao, Z. H. Lu, and J. E. Thomas, Phys. Rev. A **57**, 1427 (1998).
[32] Z. H. Lu, S. Bali, and J. E. Thomas, Phys. Rev. Lett. **81**, 3635 (1998).
[33] A. Heidmann and S. Reynaud, J. Phys. (Paris) **46**, 1937 (1985).
[34] D. F. Walls and P. Zoller, Phys. Rev. Lett. **47**, 709 (1981).
[35] L. Mandel, Phys. Rev. Lett. **49**, 136 (1982).
[36] R. Loudon, Opt. Commun. **49**, 24 (1984).
[37] Z. Y. Ou, C. K. Hang, and L. Mandel, J. Opt. Soc. Am. B **4**, 1574 (1987).
[38] M. J. Collett, D. F. Walls, and P. Zoller, Opt. Commun. **52**, 145 (1984).
[39] G. Yu. Kryuchkan, M. Jakob, and A. S. Sargsian, Phys. Rev. A **57**, 2091 (1998).
[40] M. Jakob and G. Yu. Kryuchkyan, Phys. Rev. A **58**, 767 (1998).
[41] P. R. Rice and L. M. Pedrotti, J. Opt. Soc. Am. B **9**, 2008 (1992).
[42] W. S. Smyth and S. Swain, Phys. Rev. A **53**, 2846 (1996).
[43] P. Zhou and S. Swain, Opt. Commun. **131**, 153 (1996).
[44] P. Zhou, S. Swain, and Z. Ficek, Opt. Commun. **148**, 159 (1998).
[45] L. Mandel, Phys. Rev. Lett. **49**, 136 (1982).
[46] L. Mandel and E. Wolf, *Optical Coherence and Quantum Optics* (Cambridge University Press, Cambridge, 1995).
[47] S. P. Goreslavskij and Y. P. Krainov, Opt. Spektrosk. **47**, 825 (1979) [Opt. Spectrosc. **47**, 457 (1979)].
[48] S. P. Goreslavskij, N. B. Delone, and Y. P. Krainov, J. Phys. B **13**, 2659 (1980).
[49] B. V. Kryzanovsky and A. O. Melikian, Opt. Commun. **38**, 1077 (1979).
[50] G. Yu. Kryuchkyan, Opt. Commun. **54**, 19 (1985).
[51] S. Feneuille, J. Phys. B **7**, 1981 (1974).
[52] P. Tombesi and D. Vitali, Phys. Rev. A **50**, 4253 (1994).
[53] N. Lutkenhaus, J. I. Cirac, and P. Zoller, Phys. Rev. A **57**, 548 (1998).
[54] P. Zhou and S. Swain, Phys. Rev. Lett. **82**, 2500 (1999).
[55] S. L. Mielke, G. T. Foster, and L. A. Orozco, Phys. Rev. Lett. **80**, 3984 (1998).
[56] S. Swain and B. J. Dalton, Opt. Commun. **147**, 187 (1998).
[57] R. Short and L. Mandel, Phys. Rev. Lett. **51**, 384 (1983).
[58] D. F. Walls and G. J. Milburn, *Quantum Optics* (Springer-Verlag, New York, 1994).
[59] Q. A. Turchette, N. Ph. Georgiades, C. J. Hood, and H. J. Kimble, Phys. Rev. A **58**, 4056 (1998).